Taylor & Francis
Taylor & Francis Group

ORIGINAL RESEARCH

🔓 OPEN ACCESS

Dendritic cell-derived exosomes as maintenance immunotherapy after first line chemotherapy in NSCLC

Benjamin Besse[a,b,c,*], Mélinda Charrier[a,c,d,e,*], Valérie Lapierre[a,f], Eric Dansin[g], Olivier Lantz[e,h,i], David Planchard[b], Thierry Le Chevalier[b], Alain Livartoski[j], Fabrice Barlesi[k], Agnès Laplanche[l], Stéphanie Ploix[e], Nadège Vimond[d,e], Isabelle Peguillet[e,h,i], Clotilde Théry[c,i], Ludovic Lacroix[m,n], Inka Zoernig[o], Kavita Dhodapkar[p,q], Madhav Dhodapkar[q,r,s], Sophie Viaud[a,c,t], Jean-Charles Soria[a,c,u,v], Katrin S. Reiners[w], Elke Pogge von Strandmann[w], Frédéric Vély[x,y,z,aa], Sylvie Rusakiewicz[a,e,t], Alexander Eggermont[a,c,t], Jonathan M. Pitt[a,c,t], Laurence Zitvogel[a,c,e,t,*], and Nathalie Chaput[a,d,e,f,*]

aGustave Roussy Cancer Campus, Villejuif, France; bDépartement de Médecine Oncologique (Unité thorax), Gustave Roussy Cancer Campus, Villejuif, France; cFaculté de médecine, Université Paris Sud, Le Kremlin-Bicêtre, France; dLaboratoire d'Immunomonitoring en Oncologie, UMS 3655 CNRS / US 23 INSERM Gustave Roussy Cancer Campus, Villejuif, France; eCentre d'Investigation Clinique en Biothérapies (CICBT) 1428, Villejuif, France; fLaboratoire de Thérapie Cellulaire, Gustave Roussy Cancer Campus, Villejuif, France; gDépartement d'oncologie générale, CLCC Oscar Lambret, Lille, France; hLaboratoire d'Immunologie Clinique, Institut Curie, Paris, France; iInserm U932, Institut Curie, Paris, France; jInstitut Curie, Département de médecine oncologique, Paris, France; kService d'Oncologie Multidisciplinaire & Innovations Thérapeutiques, Université Aix Marseille, Assistance Publique Hôpitaux de Marseille, Marseille, France; lDépartement de Biostatistique et d'épidémiologie, Gustave Roussy Cancer Campus, Villejuif, France; mDépartement de biologie et pathologie médicale, Gustave Roussy Cancer Campus, Villejuif, France; nLaboratoire de Recherche Translationnelle, UMS 3655 CNRS / US 23 INSERM Gustave Roussy Cancer Campus, Villejuif, France; oDepartment of Medical Oncology, National Center for Tumor Diseases (NCT) and Heidelberg University Hospital, Heidelberg, Germany; pDepartment of Pediatrics, Yale School of Medicine, Yale University, New Haven, CT, USA; qYale Cancer Center, Yale School of Medicine, Yale University, New Haven, CT, USA; rDepartment of Medicine, Yale School of Medicine, Yale University, New Haven, CT, USA; sDepartment of Immunobiology, Yale School of Medicine, Yale University, New Haven, CT, USA; tINSERM, U1015, Villejuif, France; uINSERM, U981, Villejuif, France; vDépartement d'Innovation Thérapeutique et d'Essais Précoces, Gustave Roussy Cancer Campus, Villejuif, France; wDepartment of Internal Medicine I, University Hospital of Cologne, Cologne, Germany; xCentre d'Immunologie de Marseille-Luminy, UM2 Aix-Marseille Université, Case 906, France; yINSERM, U1104, Marseille, France; zCNRS, UMR7280, Marseille, France; aaLaboratoire d'immunologie-Hôpital de la Conception, Assistance Publique – Hôpitaux de Marseille, Marseille, France

ABSTRACT

Dendritic cell-derived exosomes (Dex) are small extracellular vesicles secreted by viable dendritic cells. In the two phase-I trials that we conducted using the first generation of Dex (IFN-γ-free) in end-stage cancer, we reported that Dex exerted natural killer (NK) cell effector functions in patients. A second generation of Dex (IFN-γ-Dex) was manufactured with the aim of boosting NK and T cell immune responses. We carried out a phase II clinical trial testing the clinical benefit of IFN-γ-Dex loaded with MHC class I- and class II-restricted cancer antigens as maintenance immunotherapy after induction chemotherapy in patients bearing inoperable non-small cell lung cancer (NSCLC) without tumor progression. The primary endpoint was to observe at least 50% of patients with progression-free survival (PFS) at 4 mo after chemotherapy cessation. Twenty-two patients received IFN-γ-Dex. One patient exhibited a grade three hepatotoxicity. The median time to progression was 2.2 mo and median overall survival (OS) was 15 mo. Seven patients (32%) experienced stabilization of >4 mo. The primary endpoint was not reached. An increase in NKp30-dependent NK cell functions were evidenced in a fraction of these NSCLC patients presenting with defective NKp30 expression. Importantly, MHC class II expression levels of the final IFN-γ-Dex product correlated with expression levels of the NKp30 ligand BAG6 on Dex, and with NKp30-dependent NK functions, the latter being associated with longer progression-free survival. This phase II trial confirmed the capacity of Dex to boost the NK cell arm of antitumor immunity in patients with advanced NSCLC.

Abbreviations: APCs, antigen presenting cells; DTH, delayed type hypersensitivity; Dex, dendritic cell-derived exosomes; DC, dendritic cells; ECOG, Eastern Cooperative Oncology Group; EV, extracellular vesicles; GIST, gastroIntestinal stromal tumors; CIITA, IFN-g-inducible class II transactivator; NK, natural killer; NSCLC, non-small cell lung cancer; OS, overall survival; PS, performance status; PHA, phytohemagglutinin; PFS, progression-free survival; Treg, regulatory T cells; RECIST, Response Evaluation Criteria in Solid Tumors; RT, room temperature; Sox2, sex-determining region Y-box 2; TAA, tumor-associated antigen

CONTACT Nathalie Chaput ✉ nathalie.chaput@gustaveroussy.fr
*These authors equally contributed to this work.
🅑 Supplemental data for this article can be accessed on the publisher's website.

Introduction

The continuing development of novel immunotherapies has revolutionized the treatment of many cancers, with the success of immune checkpoint blockade strategies being a prominent example.[1,2] The goal of cancer immunotherapy is to induce tumor-targeting immunity or to strengthen an ongoing antitumor host immune response that is otherwise ineffective (e.g., following immunosuppression in the tumor microenvironment). Strategies that can harness dendritic cells (DC) or their functions, which drive tumor-associated antigen (TAA)-specific T cell responses, are therefore well positioned to achieve this end. Indeed, adoptive transfer of TAA-loaded mature autologous DCs have been described to prolong OS in metastatic castration-resistant prostate cancer patients.[3] Nevertheless, DC-based immunotherapy is often difficult to implement in a clinical setting, thus alternative and more effective vaccine strategies targeting the DC axis are sought.[4]

The use of DC-derived exosomes (Dex) is one strategy we and others have actively investigated in preclinical and clinical settings. Dex are 50–150 nm diameter secreted extracellular vesicles, generally recovered by high-speed ultracentrifugation and displaying a molecular composition that bestows them with potent immunostimulatory properties. Dex maintain the key functions of DCs in their ability to present TAAs and to activate TAA-specific immune responses.[4,5] The outer membrane of Dex contains a wide range of antigen presentation (MHC class I, class II, CD1), adhesion (ICAMs), costimulatory (CD86, CD40), and docking (integrin) molecules, each of which facilitate the in vivo functionality of Dex.[4,5] Their long-term stability after freezing, their high density in MHC peptide complexes that can be transferred to surrounding antigen presenting cells (APCs), and their potential to trigger NK cells through membrane-bound IL-15/IL-15Rα and NKG2D ligand exposure,[6] suggest potential for Dex immunotherapy approaches. Hence, over the last decade, Dex have been developed as clinical cell-free cancer vaccines.[7,8]

Phase I clinical trials using autologous TAA-loaded Dex have been previously completed in cancer patients by ourselves and others.[9,10] These two studies highlighted the feasibility of large-scale Dex production, and confirmed an excellent safety profile for Dex administration in patients. In our study, MAGE antigen-loaded Dex therapy in 15 MAGE3$^+$ advanced melanoma patients (receiving four Dex vaccinations at weekly intervals) resulted in an objective response in one patient who had a continued stability of disease for 24 mo with Dex therapy continuation. We also observed one minor response, and two stabilizations of disease.[9] MAGE-specific T cell responses were not detectable in peripheral blood, although enhanced NK cell effector functions were observed in 8 out of 13 patients.[9] In the second study,[10] 3 out of 9 patients with advanced MAGE$^+$ NSCLC who received MAGE3.A1-loaded Dex (of four vaccinations at weekly intervals) successfully developed MAGE3.A1-specific systemic immune responses as determined by delayed type hypersensitivity (DTH) reactivity, although only minimal increases in peptide-specific T cell activity were detected. NK cell lytic activity was however upregulated, in similarity with the other trial. The trial concluded with an observed stability of disease in some of the immunized patients.[10]

The backbone treatment of advanced NSCLC patients is based on four to six cycles of platinum-based doublet therapy. Although improving survival and quality of life, compared to best supportive care, its toxicity remains a challenge and alternative strategies are intensively explored.[11] Among these, attention has focused on prolonging first-line therapy benefit, in a strategy described as the 'maintenance' strategy. To date, the approved therapeutic sequence includes prolongation of one or more of the drugs used in the inducting regimen (continuation maintenance), or the introduction of another agent with no cross-resistance (switch maintenance or early second-line).[12] Immunotherapies fit the maintenance setting if their efficacy to toxicity ratio is positive, which has not been evidenced so far.[13] Due to its minimal toxicity, Dex as an immunotherapy is an appealing option in the maintenance setting to improve PFS and OS with no adverse effects on patient quality of life.

Since the phase I Dex trials, new ways to improve Dex as an immunotherapy have been established with hope to enhance the limited Dex-induced T cell responses. An important innovation here has been the use of exosomes derived from TLR4L- or interferon (IFN)-γ-matured DCs, following discoveries that such Dex induce greater T cell stimulation compared to Dex from immature DCs.[14–17] From this, we have developed a 'second generation' of Dex immunotherapy for clinical study,[16] which we hypothesized would improve upon the limited T cell-based immune responses observed in the phase I studies. In this phase II clinical trial, our primary objective was to investigate whether second generation Dex (IFN-γ-Dex) used as maintenance immunotherapy could improve the rate of PFS at 4 mo post platin-based chemotherapy in unresectable NSCLC patients.

Results

Patient characteristics

Twenty-six HLA-A2 positive patients were registered to the trial from May 2010 to April 2013 from four centers based in France: Gustave Roussy (21 patients), Institut Curie (2 patients), Oscar Lambret Institute (2 patients) and Assistance Publique Hôpitaux de Marseille (APHM) Hôpital Nord (1 patient). Four patients could not receive Dex therapy due to failures in Dex manufacturing (2 patients), death (1 patient), or progression before the first IFN-γ-Dex injection (1 patient). These four patients were excluded from further analyses (except for the characterization of IFN-γ-Dex product in two cases). Characteristics of the 22 patients are shown in Table 1. Patients were predominantly male (68%) with a median age of 62 y [range, 23–79 y]. 18 patients (82%) presented a stage IV NSCLC at diagnosis. Histology revealed 64% of patients had adenocarcinomas. All patients received a first line platinum-based chemotherapy (4 cycles), 14 patients (64%) showed stabilization while 8 patients (36%) experienced a partial response.

Characteristics of IFN-γ-Dex products

Thirty-six preparations of IFN-γ-Dex exhibiting the phenotypic characteristics summarized in Table 2 and Figure 1 were produced at the Gustave Roussy cell therapy facility. IFN-γ-Dex

Table 1. Patient characteristics.

	Frequency N = 22(%)
Gender	
Male	15(68%)
Female	7(32%)
Age	
Median	62
Range	23–79
Histology	
Adenocarcinoma	14(64%)
Squamous	4(18%)
Large Cell	3(14%)
Others	1(5%)
Stade	
IIIB	4(18%)
IV	18(82%)
Response after chemotherapy	
Partial response	8(36%)
Stable	14(64%)
Active brain metastases or carcinomatous meningitis	
No	22(100%)
Metastases	
Yes	22(100%)
Metastasis localization	
Pleura	3(14%)
Lung	14(64%)
Liver	4(18%)
Bones	11(50%)
Adrenal gland	4(18%)
Lymph node	6(27%)
Other	8(36%)
Smoking status	
Smoker	5(23%)
Non-smoker	4(18%)
Former smoker	13(59%)

release criteria were based on their expression of MHC class II molecules and tetraspanins (a >5-fold increase compared with the isotype control mAbs). Dex were also defined according to the membrane expression of co-stimulatory and adhesion molecules (Fig. 1A, left and middle panels). 75% of IFN-γ-Dex preparations exhibited a mature phenotype (>2-fold increase of CD40, CD86 and ICAM-1/CD54 compared with isotype control mAbs, Fig. 1A, right panel). IFN-γ-Dex MHC-II expression correlated with the total protein content of Dex preparations (Fig. 1B). To verify that IFN-γ-Dex MHC class I expression correlated with the total protein content of Dex

Table 2. IFN-γ-Dex vaccine characteristics.

Number of Injections	
Median	7
Range	1–27
Exosomal protein quantity (μg)	
Median	1,93
Range	99–26,648
Exosomal protein quantity/injection (μg)	
Median	247
Range	53–2,422
Cumulated exosomal protein (μg)	
Median	229
Range	375–20,333
MHC II quantity/injection	
Median	4.805×10^{12}
Range	8.5×10^{11}–1.0×10^{13}
Cumulated exosomal MHC II dose (numbers of molecules)	
Median	4.04×10^{13}
Range	1.26×10^{13}–1.67×10^{14}

molecules were loaded with MART1 epitopes, we incubated IFN-γ-Dex with a HLA-A2 restricted, MART-1 specific CTL clone (LT11), with or without HLA-A2 negative antigen presenting cells (DC). As previously described, IFN-γ-Dex transferred onto DC were able to strongly activate LT11 cells (Fig. 1C). Thirty-two batches of IFN-γ-Dex went through these quality control specifications and were released. Batch release was not validated for four productions, two batches harvested from the same patient having no Dex (patient finally excluded from the trial), one with a small amount of Dex (that was insufficient for four injections; a second successful production was made for this patient) and one with low tetraspanin expression (thus the final product could not be considered as Dex; a second successful production was made for this patient). Altogether, the feasibility of IFN-γ-Dex manufacturing was excellent, averaging 89% in this multicenter trial. Among the 22 patients that received IFN-γ-Dex injections, 13 patients received less than 9 injections due to disease progression, and 9 patients received 9 or more injections. The median of IFN-γ-Dex injections was 7 (range, 1–27). Safety of IFN-γ-Dex therapy was acceptable; 82%, 9%, 5% and 5% exhibiting zero, grade 1, grade 2 and grade 3 (elevation of ALT) toxicity, respectively.

Clinical efficacy of IFN-γ-Dex

Twenty-two patients were evaluated for clinical responses according to RECIST criteria after four injections of IFN-γ-Dex, and 10 patients (45%) were evaluated after nine injections of IFN-γ-Dex. Seven patients (32%) remained stable after nine injections, these patients continued to receive injections every three weeks. The PFS rate at 4 mo was 32% (95% CI: 16–53) and the median PFS for all 22 patients was 2.2 mo (Fig. 2A). There was no objective tumor response according to RECIST criteria. The median OS for all patients was 15 mo (Fig. 2B) with a survival rate at 6 mo of 86% (95% IC: 67–95), at 1 y of 55% (95% IC: 35–73), and at 2 y of 25% (95% IC: 11–47). One patient with a cT2N2M1b lung adenocarcinoma experienced a long-term stabilization (Patient #037; 17.6 mo). This 63-y-old male patient, a former smoker, had only two metastases, one in the brain and the other in the bone (T11). He first received four cycles of cisplatin/pemetrexed (09/2012 to 12/2012), promoting the complete regression of the brain metastasis, then entered the trial. He received 27 injections of Dex until May 2014. Considering the absence of new metastatic lesions, he underwent a right upper lobectomy in June 2014, which enabled pathologists to stage this malignancy as pT2aN2 eligible for local adjuvant thoracic and vertebral radiotherapy. CT scans or MRI at diagnosis, post-chemotherapy, and post-IFN-γ-Dex maintenance therapy are shown for the thoracic, brain and vertebral lesions in Figure 2C–E. There were no treatment-related deaths and lethal events were all disease-related.

IFN-γ-Dex did not induce cancer-specific T cell immune responses

The longitudinal study of fresh blood leukocytes revealed that IFN-γ-Dex had no impact on proportions, absolute numbers nor phenotype of the most representative peripheral blood
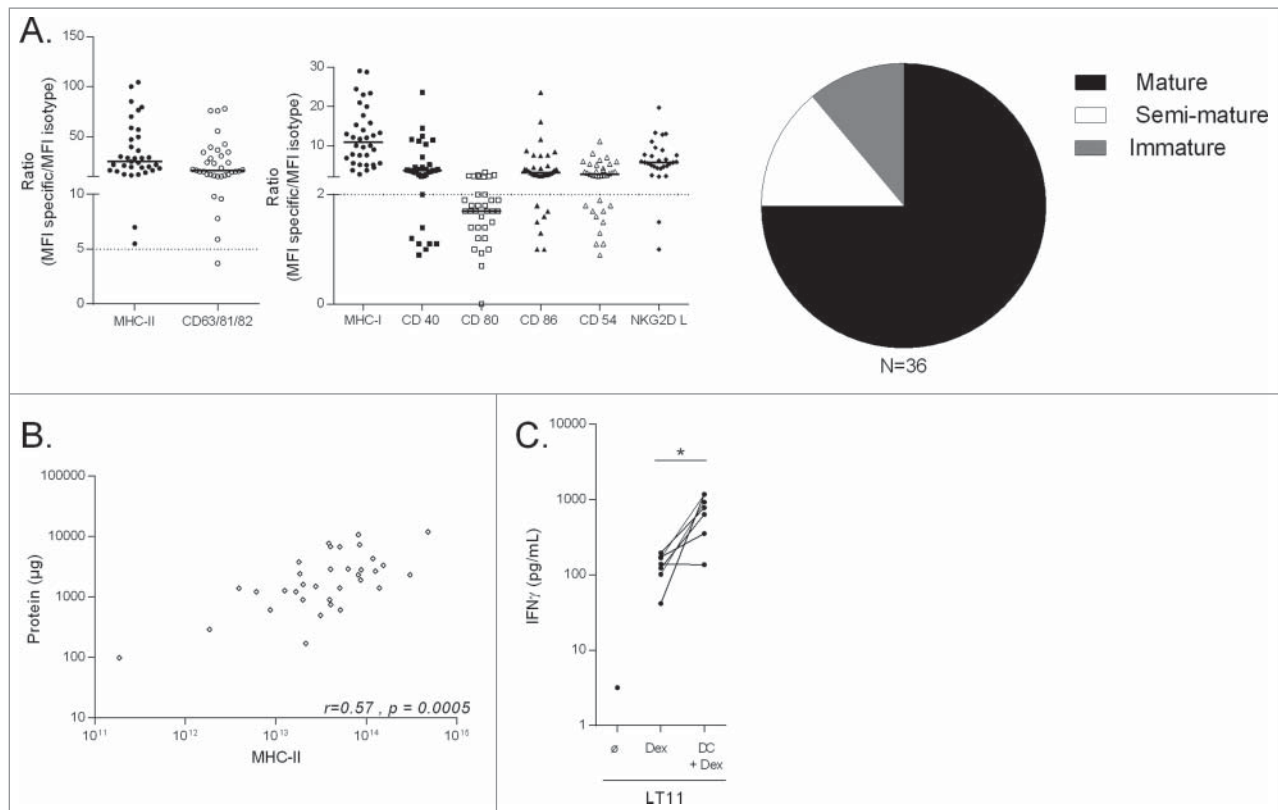
Figure 1. Quality Control of IFN-γ-Dex vaccines. (A) Thirty-six batches of IFN-γ-Dex were produced and characterized by flow cytometry after capture on beads for surface expression of MHC-I, MHC-II, tetraspanins, CD40, CD80, CD86, CD54 and NKG2DL. MHC-II and total tetraspanin (CD63/81/82) expressions represented the key parameters for Dex definition and batch release (left panel) and were considered of potential therapeutic value when the ratio of MFI for MHC-II and tetraspanin compared with the isotype control mAb was > 5 (dotted line). Dex maturity is depicted in the pi-chart (right panel) summarizing the raw data of the middle panel indicating Dex MFI ratios for each parameter compared with its isotype control mAb. Dex were considered mature if the MFI ratio of CD40, CD80 and CD86 were all > 2 compared to isotype control staining, semi-mature if at least one of these markers was > 2, and immature when all three markers were < 2. (B) Spearman correlation between total protein content of Dex preparations and Dex MHC-II surface expression. Each dot represents one patient preparation. (C) Validation of MART-1 peptide presentation on Dex surface: HLA-A2$^+$ Dex were pre-incubated (or not) with HLA-A2 negative DCs prior to incubation with the HLA-A2-restricted, MART-1-specific LT11 clone. IFN-γ levels were determined by commercial ELISA from the 48h-culture supernatants. Each dot represents a mean of duplicate wells for individual patient Dex preparations. A paired t-test of the antigenicity of Dex alone versus Dex pulsed onto DC indicates significant results at $p < 0.05$.

mononuclear cells, including monocytes, granulocytes, CD4$^+$ and CD8$^+$ T cells, Treg, $\gamma\delta$ cells, NK cells, and B cells (Fig. S1 and data not shown). T cell responses to the tumor antigens (MAGE1, MAGE3, NY-ESO1) or stem cell-associated antigen (Sox2) expected to be presented by Dex or following antigen spreading were analyzed over time in eight and ten patients respectively. T cell responses to cancer testis antigens assessed by flow cytometry on circulating CD8$^+$ T cells using specific tetramer staining were detectable (>2-fold increase compared with baseline) post IFN-γ-Dex only in two of eight cases (Fig. S1B). T cell responses to Sox2 long peptides (as defined in [18]) did not appear to be triggered by IFN-γ-Dex, but it is noteworthy that in 50% of cases, T lymphocyte responses to positive controls (virus epitopes and PHA) dropped during IFN-γ-Dex, likely in relation to disease progression (Fig. S1C). Not surprisingly, antibody responses to cancer testis antigens did not increase with IFN-γ-Dex (Fig. S1D). Altogether, no clear induction of adaptive immune responses could be monitored after IFN-γ-Dex injections.

IFN-γ-Dex increases NKp30-related NK cell functions

Two phase I trials assessing the feasibility and safety of Dex therapy exemplified an NK cell-specific bioactivity of Dex in

melanoma and NSCLC patients, who experienced enhanced NK cell cytolytic functions post-Dex therapy.[6,9,10] In the current phase II trial, we observed a weak expression of NKp30 and a slight drop in CD16 expression on circulating NK cells in most NSCLC patients, this contrasting with the healthy age-matched cohort with normal/high levels of NKG2D receptors (Fig. 3A and Fig. S2A). Nevertheless, longitudinal study of these receptors on NK cells from fresh whole blood showed that IFN-γ-Dex injections could not modify the proportion nor the MFI of NKp30, CD16, or NKG2D (Fig. S1). Longitudinal phenotyping of thawed NK cells showed no modification of the proportion nor the MFI of NKp30 (as compared with fresh whole blood) but significantly increased CD16 expression levels by T2 (Fig. 3B) which differs from observations made on NK cells from fresh whole blood. Of note, surface expression of NKG2D was negative (endocytosis) after thawing and overnight culture of PBMC. We then studied NK cell effector functions on thawed PBMC by cross-linking NKp30 or CD16 receptors (used as a positive control) in 13 patients at baseline (T0) and after 4 IFN-γ-Dex injections (T2) (Fig. 3C and Fig. S2). Despite the low expression levels of surface NKp30, NKp30 cross-linking led to a significant augmentation of the proportions of IFN-γ^+ and IFN-γ^+TNFα^+ secreting NK cells after four IFN-γ-Dex
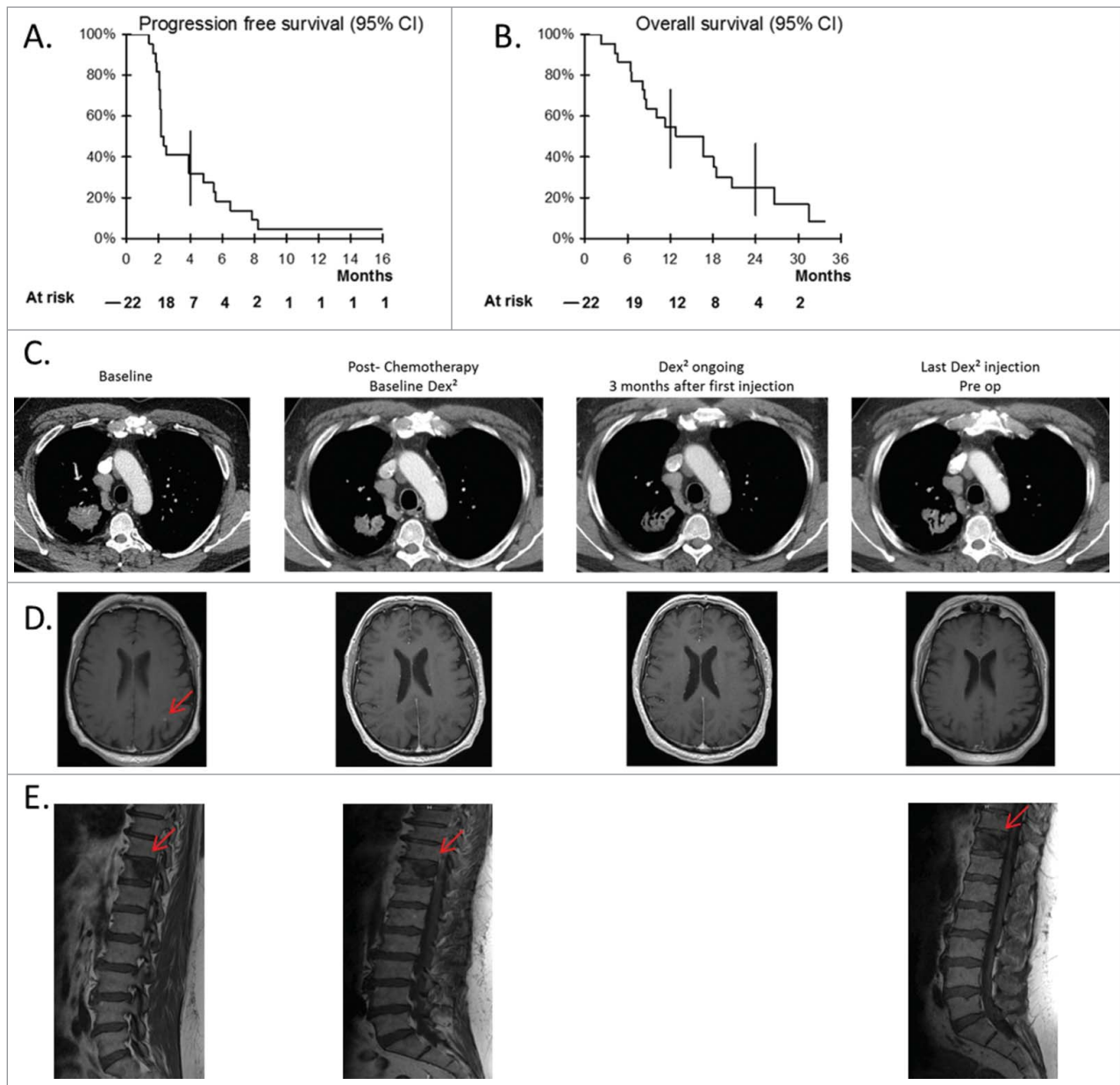
Figure 2. Clinical responses to Dex vaccination post-chemotherapy. Progression free survival (A), and OS (B) of the cohort of 22 patients recruited into the trial (95% confidence interval). (C–E) Case report of patient 037. Thoracic (C) and brain (D) CT scans as well as a longitudinal follow up by MRI of the 11th dorsal vertebra (E) are shown for the best clinical response obtained in one patient with a stage IV NSCLC. Imaging at baseline (before-chemotherapy), post-chemotherapy (before commencement of Dex injections), at 3 mo after the first Dex injections, and at the last Dex injection before surgery of the thoracic lesion.

vaccines (Fig. 3C). A boost of NK cell functions was also observed with CD16 cross-linking (Fig. S2C), consistent with the augmentation of CD16 expression levels by T2 on thawed NK cells (Fig. S2C). To further analyze whether NKp30 cell functions could correlate with clinical parameters, we separated the patients into two groups based on the median PFS (Fig. 3D). After four IFN-γ-Dex injections (T2), a significant increase in CD107a$^+$ NK cells was observed only in those patients with a PFS over 2.2 mo (Fig. 3D). Notably, patient #037, who experienced long stabilization, showed a great increase in NK cell function after Dex injection (Fig. 3D, indicated by red dots). None of the T cell parameters presented in Fig. S1 were associated with PFS (not shown).

Correlations between phenotypic traits of IFN-γ-Dex vaccines and NKp30 activation *in vivo*

We describe an augmentation of NK cell function after IFN-γ-Dex injections in patients experiencing a longer PFS. Although we previously reported that Dex can directly trigger NK cell activation *in vitro*,[6] this observation could have many explanations unrelated to Dex injections. Therefore, we investigated whether any of the phenotypic characteristics described in Fig. 1 (protein levels, MHC-II expression and quantification, MHC-I, CD40, CD80, CD86, NKG2D-L, IL-15Rα and CD54/ICAM-1 expression) could be correlated with NK cell functions. We identified that NKp30 functions
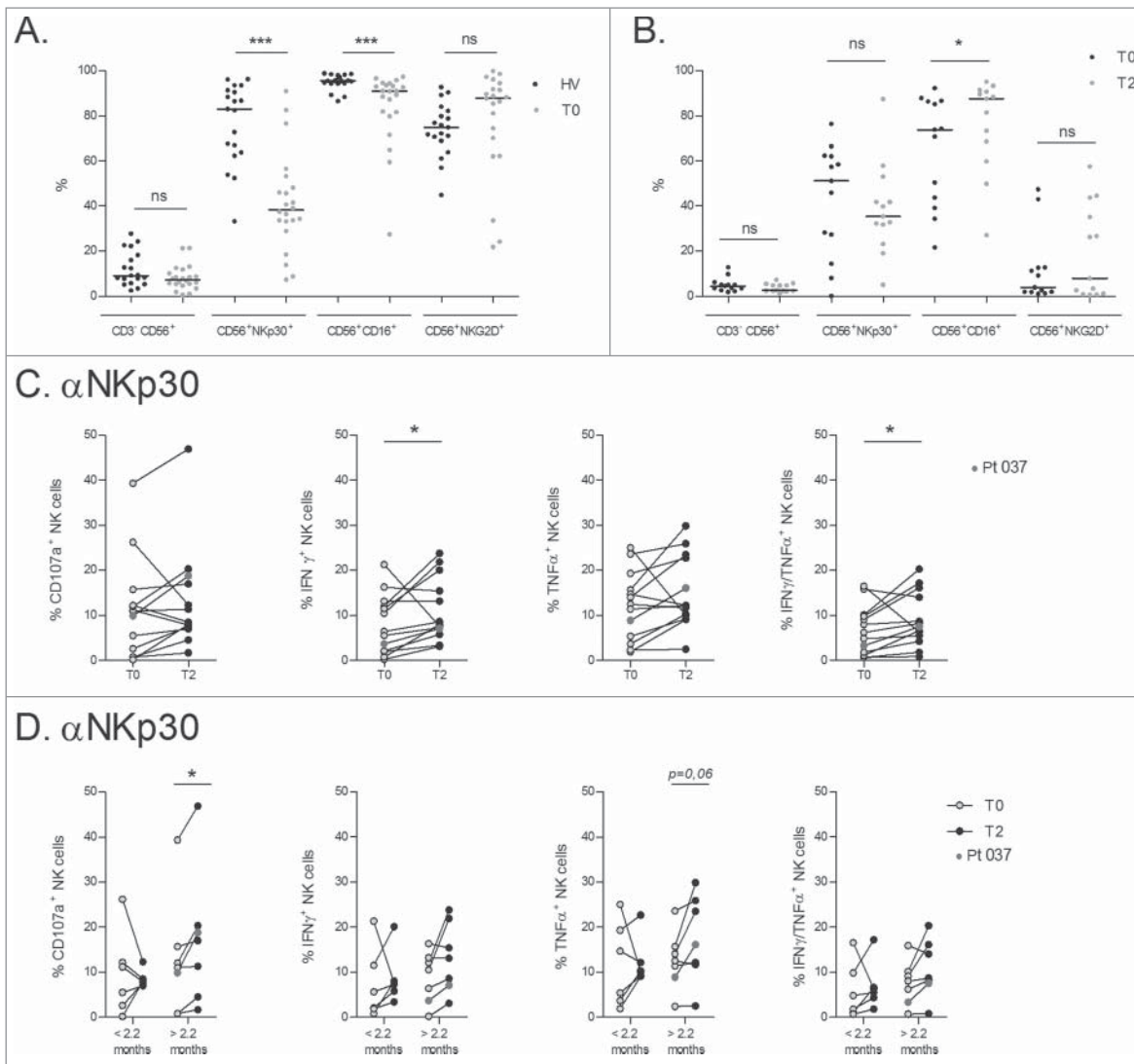
Figure 3. IFN-γ-Dex-mediated induction of NKp30 effector functions and correlation with progression-free survival. (A) NSCLC patients exhibit markedly reduced NKp30 expression on circulating NK cells. Flow cytometry determinations of expression levels of NK receptors (NKG2D, NKp30 and CD16) in the peripheral whole blood CD3$^-$CD56$^+$ NK cells of HV and NSCLC patients at their inclusion into the trial (baseline, T0). (B) Flow cytometry analyses were performed after freezing/thawing, at T0 and post 4 Dex injections (T2). (C) Flow cytometry analyses of NK cell functions after cross-linking of NKp30 as measured by CD107a upregulation and cytokine intracellular staining (at 5 h), comparing baseline (T0) and post 4 IFN-γ-Dex vaccinations (T2). (D) IFN-γ-Dex-mediated NKp30 triggering is associated with prolonged PFS. NSCLC patients were segregated into two groups according to the median PFS of the whole cohorts (< 2.2 mo, and > 2.2 mo respectively). CD107a upregulation and cytokine production following NKp30 cross-linking are shown at T0 and T2 for each subgroup. Patient #037, who experienced a long-term stabilization post Dex therapy as shown in Figure 2 is indicated with red dots. The experiment was performed in triplicate wells, the three wells were pooled before FACS staining. Each dot represents one patient. Paired *t*-test *p*-value is indicated on the graph.

were significantly increased at T2 in patients that had received higher doses of Dex associated MHC-II (Fig. 4A). Since DC maturation was induced in our process with IFNγ and this cytokine is known to induce high expression of MHC-II,[19] we determined the concentration of IFN-γ in DC preparations at D4 (before addition) and D6 (after addition of IFN-γ) as well as in the final Dex product. The GMP process of Dex harvesting implicates one step of ultrafiltration allowing the discard of proteins of less than 500 kDa in weight, as is free IFN-γ. In all DC supernatants, we indeed recovered high concentrations of IFN-γ between D4 and D6 (not shown). However, significant IFN-γ concentrations were measurable in only a few Dex preparations, likely bound to their receptors expressed on Dex external membranes. Hence, we explored if Dex-associated

IFN-γ could be associated to MHC-II quantities in the final vaccine product and found a strong correlation between these two parameters (Fig. 4B). Previous studies have shown a link between MHC-II, IFN-γ and BAG6,[20,21] the latter known to directly activate NK cells through engagement of the NKp30 receptor.[22] We identified that all 7 Dex preparations that could be evaluated by ELISA were positive for BAG6 (7.7 ng, range [3.37–17.59]). The expression of proteins of the MHC class II processing pathway is regulated by the IFN-γ-inducible class II transactivator (CIITA) at the transcription level.[21] Interestingly, IFN-γ stimulation can lead to a synchronized upregulation of CIITA and BAG6 expression, thereby coupling the expression of MHC class II molecules to BAG6.[20] We hypothesized that MHC-II quantity recovered in the final Dex preparations could be
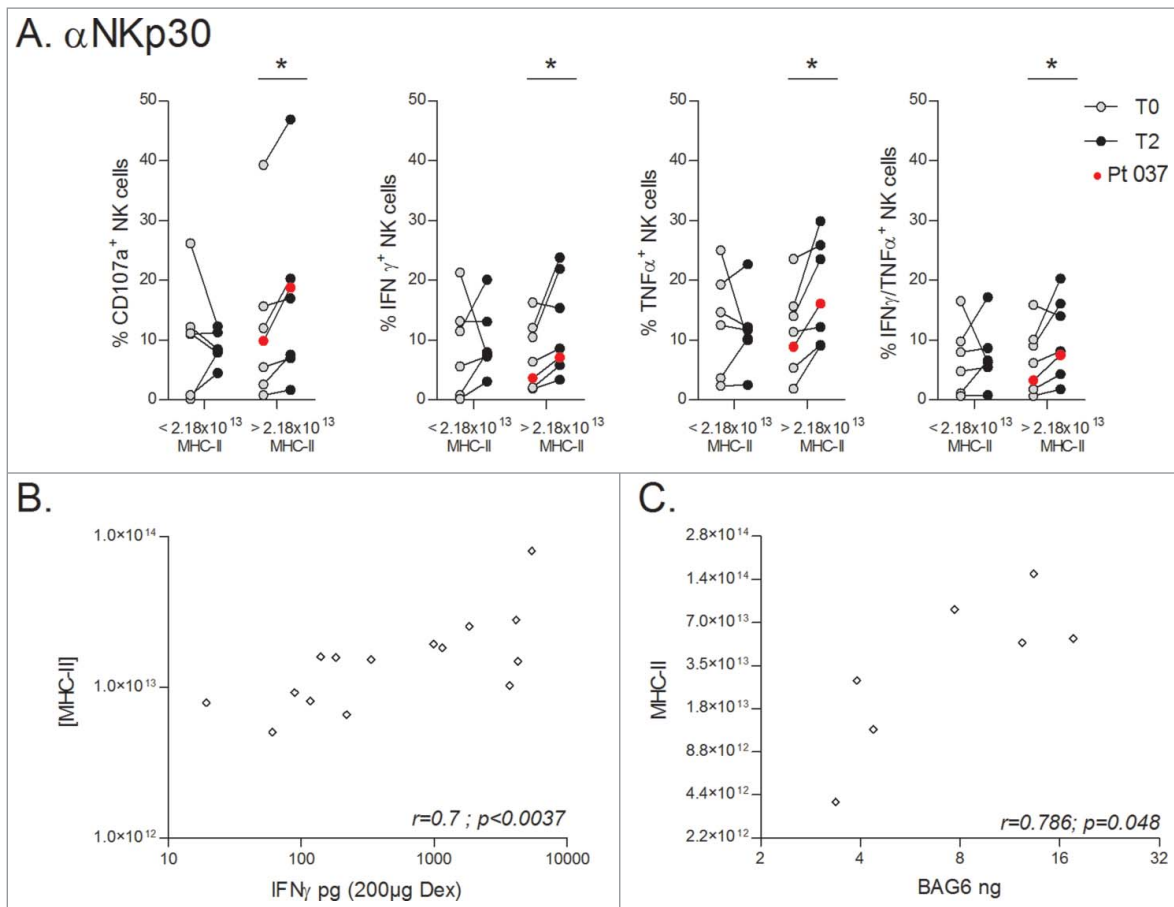
Figure 4. Dex MHC-II molecules predict BAG6 / NKp30-mediated NK cell activity. (A) Dex preparations produced for the whole cohort of NSCLC patients were divided into two groups either side of the median MHC-II quantity of 2.18×10^{13} molecules ($< 2.18 \times 10^{13}$ MHC-II, and $> 2.18 \times 10^{13}$ MHC-II respectively), and CD107a upregulation and cytokine production following NKp30 cross-linking were determined comparing baseline (T0) and post 4 IFN-γ-Dex vaccinations (T2). The experiment was performed in triplicate wells, with the three wells pooled before FACS staining. Patient #037 with long-term stabilization post-Dex therapy as shown in Fig. 2 is indicated with red dots. Paired t-test p-value is indicated on the graph. (B) Spearman correlations between IFN-γ levels (measured on Dex batches) and MHC-II quantity within the same preparations. (C) Spearman correlations between BAG6 quantity (measured by ELISA on Dex batches) and MHC-II quantity in the same Dex.

linked to BAG6. As shown in Fig. 4C, BAG6 recovered in Dex preparations was indeed positively correlated with MHC-II Dex content. Together, these data suggest that BAG6 recovered in IFN-γ-Dex preparations could activate NK cells in a NKp30-dependent fashion.

sBAG6 and NKp30 anergy in a subset of NSCLC patients

The two main NKp30 ligands known to engage the NKp30 receptor and dampen its activity when shed in the serum or in supernatants are sB7-H6 and sBAG6.[22-24] In our cohort of NSCLC patients, 60% and <10% presented detectable serum levels of sBAG6 (cut-off value, 0.5 ng/mL) and sB7-H6 (cut off value: 0.6 ng/mL) respectively (Fig. 5A, left panel). Plasma levels of sBAG6 detected in healthy volunteers (HV) had a mean concentration of 0.47 ng/mL (data not shown). Levels of sBAG6 and sB7-H6 remained constant throughout the first 4 injections (T2) of IFN-γ-Dex therapy (Fig. 5A right panel). Comparison of the NKp30 effector functions in patients presenting sBAG6 with those having undetectable sBAG6 at diagnosis (T0) revealed that the presence of this soluble marker was associated with NKp30 (but not CD16) –dependent anergy at T0 (Fig. 5B-C, left panels). sBAG6 shed in the circulation may

therefore account for part of the disabled NK cell functions observed in NSCLC patients. However, at T2 after 4 IFN-γ-Dex injections, NKp30-dependent functions were similar in this subgroup of patients regardless of detectable sBAG6 (Fig. 5B-C, right panels), suggesting that IFN-γ-Dex stimulation allowed NK cells to bypass the inhibitory effects of soluble BAG-6.

Discussion

The results of this phase II trial indicate (i) that IFN-γ-Dex is a very well tolerated immunotherapy, (ii) that effective clinical-grade IFN-γ-Dex production is feasible, (iii) that IFN-γ-Dex, when used as maintenance immunotherapy in chemotherapy-stabilized/responding NSCLC patients, boosts NKp30-dependent NK cell functions while (iv) having no detectable induction of antigen-specific T cell responses. Importantly, this Dex-induced enhancement of NK cell functions occurs in those patients benefiting from prolonged PFS and correlates with IFN-γ-Dex content of MHC class II molecules and with the presence of the NKp30 ligand BAG6 in the vaccine product.

Studies have highlighted alterations in intratumoral NK cells in Stage I-IIIA NSCLC. Platonova et al. observed a coordinated
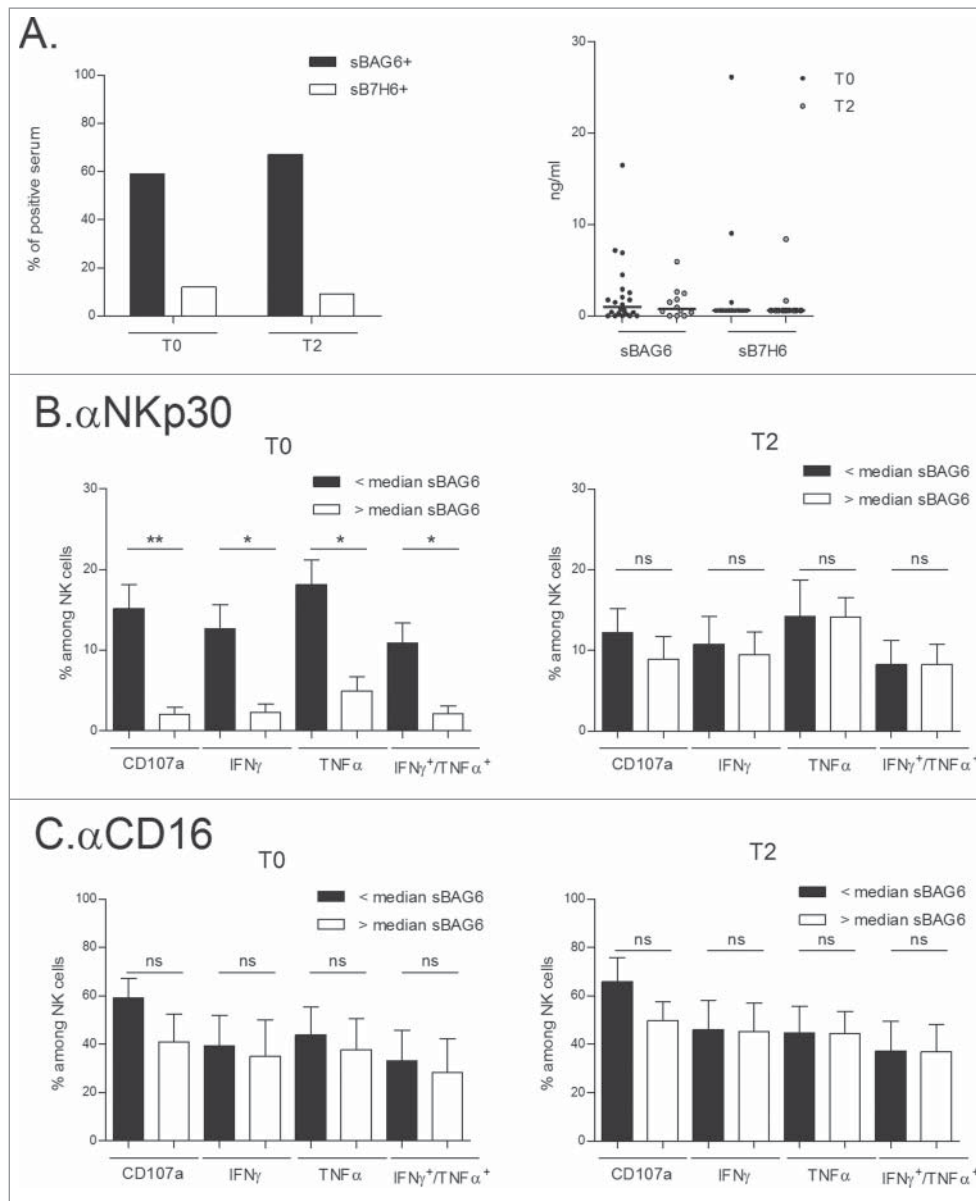
Figure 5. Circulating sBAG6 and NKp30 anergy restored by IFN-γ-Dex. (A) Monitoring of serum soluble BAG6 or soluble B7-H6 at diagnosis and T2 in NSCLC patients by ELISA expressed as percentages of positive samples (cut-off values, 0.5 ng/mL for BAG6; 0.6 ng/mL for sB7-H6) (left panel) and genuine values (right panel). (B–C) Idem as in Fig. 3 monitoring NKp30- (B) or CD16- (C) mediated effector functions in the subsets of patients presenting or not presenting detectable sBAG6 at diagnosis (T0) and (T2). Eleven patients were assessed and the means±SEM of flow cytometry values are shown. Paired *t*-test *p*-value is indicated on the graph.*$p < 0.05$.

decrease in the expression of a cluster of NKp30, NKp80, DNAM-1 and CD16 receptors in intratumoral NK cells as compared to NK cells of distant normal tissues and circulating blood NK cells.[25] The authors suggested that such local impairment of antitumor NK cell activity might contribute to cancer progression. Other studies scrutinizing NK cell infiltration in lung cancer patients have pinpointed that NK cell infiltration might be associated with longer survival.[26,27] These characterizations of NK cells however relied on CD56 or CD57 expression measured by immunohistochemistry; additionally the study by Platonova and colleagues was undertaken in operable lung cancer (stage I-III) using flow cytometry analyses. In our advanced and inoperable NSCLC (stage IIIB-IV) patients, we observed a marked decrease in NKp30 and (to a lesser extent) CD16 expression in circulating blood NK cells, indicating that at advanced stages of the disease, the alteration of NK

cells becomes systemic. In this study we searched for soluble NKp30 ligands. Soluble B7-H6 could not be readily detected while soluble BAG6 was detected in 60% of cases (Fig. 5A). Higher levels of soluble BAG6 were linked to blunted NKp30 (but not CD16)-dependent cell functions after receptor engagement (Fig. 5B). It is therefore conceivable that the secretion of BAG6 from the tumor microenvironment is responsible for impaired NK cell functions, as has been shown in other cancers.[28,29]

We investigated how IFN-γ-Dex immunotherapy could impact NK cell functions in advanced NSCLC, and were able to show that high concentrations of MHC-II and IFN-γ correlated with the highest NK cell activities. BAG6 is a ligand for the NKp30 receptor on NK cells,[22,30] and its expression is strongly linked to that of MHC-II as both are controlled by CIITA downstream of IFN-γ signaling.[20] BAG6 has been shown to be

required for HSP70 accumulation,[31,32] with HSP70 having the ability to activate NK cell cytotoxicity,[33] and HSP70 surface-positive exosomes reportedly favoring migratory and cytolytic activity of NK cells.[34] Although elevated soluble BAG6 in the serum of leukemic patients appears to correlate with impaired NK cell function,[28,29] BAG6 when expressed on the surface of exosomes has been observed as a potent activator of NK cells.[29,35] BAG6 and HSP70 have been shown to be associated with exosomes and could act coordinately to trigger NK cell activation.[35] It is therefore conceivable that exosomal membrane-associated BAG6 would be a stimulatory form of BAG6, as opposed to the suppressive soluble form of BAG6. The assumption we make is that the BAG-6/hsp70 heterodimer activates NK cells via a co-engagement of CD94 and NKp30 receptors. Thus, although the level of expression of NKp30 on the surface of NK cells and levels of soluble Bag-6 are not changed, IFN-γ-Dex$^{BAG6+(HSP70+}$ allow NK cell activation via engagement of both activating receptors. NKG2D, NKp46, NKp44 and NKp30 expression levels on whole blood NK cells were followed during this clinical trial, though we did not monitor the expression level of CD94/NKG2C on NK cells during the treatment at that time. We therefore cannot exclude that the density of CD94/NKG2C could be significantly up-regulated after treatment with IFN-γ-Dex$^{BAG6+(HSP70+}$. Indeed, some papers have shown the density of CD94 can be significantly up-regulated concomitantly with increased NK cell cytolytic activity, when NK cells are stimulated with Hsp70 protein (and even more so with Hsp70 peptide plus IL-2).[36,37] This finding is reminiscent of our previous report where IL-15Rα^+NKG2DL$^+$ Dex could activate NK cells while the soluble form of NKG2DL failed to do so.[6] Another explanation could be the oligodimerization of BAG6 when expressed on Dex (or cell) surface membranes as suggested in previous studies.[30] Our data suggest that the use of IFN-γ as a DC maturing agent in the manufacturing process of Dex was key to influencing BAG6 expression and the restoration of NKp30-dependent effector functions in this category of individuals presenting depressed NKp30 levels and/or NKp30 anergy.

Despite the intention behind the development of second generation Dex, we failed to observe a cooperation of T cells beside NK cell stimulation. This could be explained by several factors including a lack of collectable T cells in the circulation (e.g., resulting from T cell migration to tumors), heterogeneity of the advanced-stage patient cohort, or regulatory mechanisms (e.g., Treg activity) that still impede this immunotherapy. Indeed, we vaccinated patients with metastatic NSCLC, where an immunosuppressive tumor contexture may interfere with the capacity of IFN-γ-Dex to prime an antitumor immune response. In line with this, all the DC vaccine trials performed in metastatic patients have given negative results so far; the only approved DC cancer vaccine being developed in asymptomatic or minimally-symptomatic metastatic castrate-resistant (hormone-refractory) prostate cancer patients.[3] A more simple possibility is that the Dex MHC-I- and MHC-II-restricted antigens employed in our study are insufficient to generate an appropriately targeted T cell response in these NSCLC patients. Alternatively, the presence of immunoregulatory molecules such as PDL1 on the surface of IFN-γ-Dex may inhibit T cell responses, prompting the concomitant utilization of neutralizing anti-PDL1 monoclonal antibodies. Our preliminary data did not invalidate this latter possibility (not shown). Finally, the in vivo trafficking of IFN-γ-Dex to skin layers and/or secondary lymphoid organs remains unknown in patients. Instead of sufficiently reaching the T cell zones, they might also be transported to subcapsular sinus macrophages or lymphatic sinus DC to encounter innate lymphocytes.[38]

In this cohort of advanced NSCLC patients, we could not evidence any diminution of the proportion of NKG2D$^+$ NK cells compared to age-matched HV. In our previous phase I study, melanoma patients vaccinated with Dex were shown to have an augmented recirculation of NK cells with a restoration of NKG2D expression and function on these cells.[9] Dex were later confirmed to activate NK cells through NKG2D and CD122/IL-15Rα signaling.[6] Notably, the Dex immunotherapies used in this previous study were not derived from IFN-γ-maturated DCs, thus, NKG2DL- and IL-15Rα-mediated NK stimulation may have featured more prominently in the possible absence of BAG6/NKp30 signaling.

We could not meet our primary endpoint to reach 50% non-progressors by 4 mo post-chemotherapy. Several reasons may explain why Dex therapy did not fulfill our initial expectations. First, cancer-testis antigens loaded onto exosomes might not be clinically relevant. Second, IFN-γ used in the process of production may have up-regulated PD-1 ligands on Dex. Third, immunotherapy approaches like vaccines may greatly benefit from a less immunosuppressive tumor contexture, hence the use of immune checkpoint blockers being important in lung cancer. However, our current study demonstrates that activation of NK cells through NKp30 might be an effective immunomodulatory strategy for patients with stage IIIB/IV NSCLC. We postulate that IFN-γ-Dex may represent an NK cell-based immunotherapy in patients harboring NKp30-specific functional defects that occur in some cancers, such as GastroIntestinal Stromal Tumors (GIST),[39] neuroblastoma,[24] chronic lymphocytic leukemia,[29] and NSCLC as described in the present study.

Patients and methods

Patients

This study enrolled stage IIIb and IV NSCLC patients not eligible to locoregional treatment, HLA-A2$^+$ phenotype, responding to or stabilized after 4 cycles of platinum-based chemotherapy Eastern Cooperative Oncology Group (ECOG), performance status (PS) from 0 to 1, and neutrophils $\geq 1.5 \times 10^9$/L. Major exclusion criteria were: autoimmune disease requiring systemic immunosuppressive therapy, concurrent steroid or immunosuppressive therapy, active brain metastases, VEGF or EGFR treatment.

The median duration time between when patients achieved stabilization or response and when they entered the trial was one week (range 0.1 – 3 weeks). Three weeks after inclusion patients received three weeks of metronomic cyclophosphamide at 50 mg/d followed by four intradermal exosome vaccinations at one-week intervals. After a two-week break, during which the disease evolution was measured, patients received six Dex vaccinations at two-week intervals followed by two-weeks

break, before continued vaccinations at three-week intervals until progression or Dex unavailability.

Clinical responses were assessed by computed tomography scan every eight-weeks and the responses were classified according to the Response Evaluation Criteria in Solid Tumors (RECIST) criteria. Toxicity was assessed according to CTCAE version 4.

The primary endpoint was to observe at least 50% of patients with PFS at 4 mo after chemotherapy cessation. The secondary objectives of the trial were to study the clinical efficacy of Dex (assessed as OS and objective response rates), to determine biomarkers of efficacy (including restoration of NK cell receptor expression, NK cell activation, and Dex peptide-specific T cell responses), and to reevaluate the safety of IFN-γ-Dex in this patient cohort.

Healthy donors

Whole blood from 19 individuals with no tumoral disease was obtained according to a procedure validated by the CCPSL UNT-N°12/EFS/079. This cohort had the same male to female ratio and median of age (67, range [50 – 81]). Regulatory T cells (Tregs) and NK cells were monitored by flow cytometry.

Dendritic cell differentiation and Dex production/purification

As previously described,[16] MD-DC were generated from monocytes isolated by ELUTRA® (CaribianBCT, Zaventem, Belgium) from HLA-A2$^+$ patients. Monocytes were differentiated into DC by adding human rGM-CSF at 1,000 ui/mL and human rIL-4 at 200 ui/mL (Cellgenix, Freiburg, Germany). At day 4, the MHC-I peptides MAGE-A1 (KVLEY-VIKV), MAGE-A3 (KVAELVHFL), NY-ESO-1 (SLLMWITQV), Melan-A/MART1 (ELAGIGILTV) and the MHC-II peptides MAGE-A3 -DP04 (KKLLTQHFVQENY-LEY) and EBV (pan-DR; PRSPTVFYNIPPMPLPPSQL) (Synprosis, Marseille, France) were added in the culture medium (each at 1 μM), with DC maturation induced by 1,000 UI/mL rIFN-γ (lmukin®, Boehringer Ingelheim, France). To verify complete differentiation into DC and their maturation, phenotyping was performed at day 4 and day 6 by flow cytometry using a Cyan flow cytometer (Beckman Coulter®) and FlowJo analysis software (Tree Star, Inc., Ashland, USA). The percentage of contaminants was also evaluated by flow cytometry (flow cytometry reagents are detailed in Table S1). Dex secreted into MD-DC culture supernatants were isolated following a process of ultrafiltration/diafiltration and ultracentrifugation through a 1.21 g/mL sucrose cushion described by Lamparski and colleagues.[7] During the first productions, we observed the presence of a CD15$^+$ cell population after elutriation. This population was never seen during preclinical runs, clinical trials, nor during acquisition of data from the HV. Differentiation of monocytes into DCs was not affected by the presence of CD15$^+$ cells although we observed an immature phenotype of DC and Dex. Therefore, we added to the conventional manufacturing process a Ficoll gradient step (Lymphocyte Separation Medium LSM 1,077, PAA Laboratories GmbH, Pasching, Austria) when the ratio CD14$^+$/CD15$^+$ cells was lower than four before elutriation.

Dexosome immunophenotype

One μg of Dex were coupled to 4 μm aldehyde sulfate beads (Invitrogen, Pontoise, France) and stained with fluorochrome-conjugated antibodies specific for various transmembrane proteins. Dex-coupled beads were acquired by flow cytometry (Cyan, Beckman Coulter®) and analyzed using FlowJo software. Reagents used are listed in Table S1.

Determination of Dex proteins and MHC II concentration

Dex proteins were quantified by DC^{TM} Protein Assay (Bio-Rad Laboratories). As we have previously described,[16] the absolute number of MHC class II molecules per bead was determined by flow cytometry as a function of the MFI (mean fluorescence intensity). Only doses within the linear range were used for calculation. Final quantifications are expressed as numbers of MHC class II molecules per mL of Dex preparations.

Quantification of IFN-γ

IFN-γ was quantified from day 4 and day 6 MD-DC supernatants, and from IFN-γ-Dex using the Bio-Plex® MAGPIX^{TM} Multiplex assay (Bio-Rad Laboratories).

Quantification of BAG6

Detection of BAG6 was performed using the sandwich ELISA procedure. Plates were coated overnight at 4°C with mouse monoclonal 3E4 (raised against the BAG6 N-terminus) as capture antibody and blocked with 1% BSA-PBS for 1 h at room temperature (RT). Standard and IFN-γ-Dex or plasma/serum were added for 1.5 h at RT. Bound BAG6 was detected using the polyclonal chicken anti-BAG6 (13pp2, raised against recombinant BAG6 N-terminus) followed by goat anti-chicken POD. The assay was developed with 100 μL 1-step ultra TMB ELISA solution (ThermoScientific). The reaction was stopped after 20 min. with 50 μL 30% sulfuric acid, and absorbance was measured at 450 nm.

Quantification of sB7-H6

Soluble B7-H6 was detected in the sera of patients by the following ELISA method. First, 96-well Nunc-Immuno^{TM} plates (Thermo Scientific) were coated with 17B1.3 mAbs at 5 μg/mL in 0.1 M NaHCO3 solution overnight at 4°C. Blocking solution (PBS supplemented with 3% BSA) was then added overnight at 4°C. After discarding this solution, serial dilutions of sB7-H6 were incubated in each well for 3 h at RT. Then, biotin-conjugated B7-H6 was added to each well (1 μg/mL in PBS supplemented with 1% BSA) for 1 hour at RT. Anti-biotin HRP (Sigma Aldrich) was then added for 1 h at RT. Finally, BD Optia TMB substrate (BD Biosciences) was used to reveal the staining and left to incubate for 15–30 min at RT. The reaction was stopped with 1 M HCl, and the Optical Density (OD) at 450 nm was read using an Apollo LB 911 (Berthold). The threshold of sB7-H6 detection in our ELISA was 0.6 ng/mL. In a cohort of healthy individuals, sB7-H6 serum concentrations were below 3 ng/mL.[23]

Antibody responses to cancer testis antigens

The multiplex analysis with *in situ* purified GST-tag fusion proteins based on the Luminex technology was performed in 96-well plates as previously described[40] Briefly, for each antigen

(Mage A1, Mage A3, MelanA, NY-ESO-1) and bead set, 3,000 glutathione-casein-coated beads per serum sample were used and sera were measured at 1:1,000 dilutions in triplicates. Reporter fluorescence of the beads was determined with the Bio-Plex analyzer (Biorad) and expressed as median fluorescence intensity (MFI) of at least 100 beads per set per well. Antigen specific reactivity was calculated as the difference between antigen-MFI and GST-tag-MFI. The median of the three triplicate MFI values for each TAA and each serum sample was used for further analyses. Primary data analyses were performed with Microsoft Excel (Office 2004). A cut-off, calculated for each antigen based on mean values plus three times the standard deviation, was used to determine sero-positive samples of the 26 healthy individuals. For cut-offs below MFI = 50, the cut-offs are adjusted to 50 due to limitations of the Bio-Plex Analyzer for low MFI and fluorescent background.

Detection of SOX2 and CEF (viral)-specific T cells

Frozen PBMCs obtained prior to and after therapy were thawed together, rested for two hours at 37°C and then washed and re suspended in 5% PHS (RPMI with 5% pooled human serum) with 2 U/mL of IL-2. The cells were plated at 0.25 million cells per well in a 96 well round bottom plate and cultured either alone (negative control) or with overlapping peptides from SOX2 antigen at 5 μg/mL. Peptide mix from viral antigens (CEF; cytomegalovirus, Epstein Barr, Influenza virus; 2.5 μg/mL) and PHA (phytohemagglutinin) were used as positive controls. After 48 h of culture, the cell supernatant was harvested and examined for the presence of CXCL10 (also known as IP-10) using a luminex assay as previously described.[18,41] Overlapping peptide library covering the entire length of the SOX2 protein has been previously described.[41] The pool of viral antigens (CEF) was purchased from Anaspec Inc., San Jose, CA.

Specific tetramer stainings

Frozen peripheral blood leukocytes (PBL) were thawed and washed in HSA (0.4 g/L) CO_2 independent (Invitrogen) medium before incubation for 1 h with DNAase (10 μg/mL) in the same medium at RT. The cells were then stained with BMFL1 (EBV) (GLCTLVAML) APC-conjugated HLA-A2 tetramers and one of the following PE-conjugated HLA-A2 tetramers all at 20 nM: Melan-A (ELAGIGILTV); MAGE-A3 (KVAELVHFL); MAGE-A1 (KVLEYVIKV), NY-ESO-1 (SLLMWITQV). All tetramers were kindly provided by D. Coleau from LICR, Brussels. After a 30 min incubation at RT, the cells were incubated with anti-CD45RO-Alexa-700 (Becton-Dickinson), anti-CD8β-PE-Cy5.5 (Beckman-Coulter), anti-CD5-FITC (BD), anti-CD4$^+$-PE-Texas-Red, and anti-CD27-Qdot-605 (Invitrogen) for 30 min. After further washes, the cells were acquired on a Canto-B (Becton Dickinson) and analyzed using FlowJo software (Tree-star).

In vitro T cell assay to assess the functionality of MART-1 peptide-loaded exosomes

As previously described,[16] increasing amounts (from 1 to 30 μg) of exosomes were pre-incubated 2 h at 37°C with 2 × 10^4 DC before adding 2 × 10^4 MART-1-specific, HLA-A2-restricted LT11 clonal cells per well. HLA-A2$^+$ and HLA-A2$^-$ DC were pulsed with 1–10 μg/mL of MART1 before incubation

with LT11 as controls of each experiment. Cultures were performed in V-shaped 96-well plates using RPMI complete medium supplemented with 10% human pooled AB serum in a final volume of 200 μL/well, for 48 h at 37°C. Supernatants taken at 48 h of incubation were assayed for IFN-γ by ELISA (R&D systems, Lille, France).

Immunomonitoring of peripheral leukocyte phenotype, T cell and NK cell functional evaluations

Blood samples were collected at different timepoints i.e. at inclusion (T0), after one month of cyclophosphamide (T1), after 4 Dex vaccinations (T2), after 10 Dex vaccinations (T3), and at the end of the study (Tf). Phenotyping was performed on whole blood, with PBMC isolated by Ficoll density gradient and frozen for later analyses. Whole blood was incubated with fluorochrome-conjugated antibodies (see Table S1) for 15 min at RT, followed by 15 min of lysis (FACS Lysis Buffer, BD). Stained cells were acquired using a Canto II flow cytometer (BD) and analyzed using FlowJo software. Tregs, mucosa-associated invariant T (MAIT) cells, NK cells and monocytes were monitored.

Evaluation of NK cell effector functions

Ninety-six-well Maxisorp® plates were coated with anti-CD16 monoclonal antibodies (mAbs) (clone 3G8, BioLegend), anti-NKp30 mAbs (clone 210847, R&D), or the respective isotype control mAbs (each at 2.5 μg/mL in 50 μL of sterile PBS 1X). Plates were incubated overnight at 4°C. Thawed PBMC were incubated overnight with Cellgro medium (Cellgenix) at 2 × 10^6 cells/mL. The next day, cells were incubated in the antibody-coated plates for 5 h in the presence of anti-CD107a, IL-2 (1,000 iu/mL), and Brefeldin A. Cells were then stained with anti-CD3 (BW264/56), anti-CD56 (N901), anti-CD45 (J33) and LIVE/DEAD® fixable yellow dead cell dye (Molecular Probes, Life Technologies). For intracellular staining, cells were fixed and permeabilized according to the Cytofix/Cytoperm™ protocol (BD Bioscience) and then stained with anti-IFN-γ (4SB3) and anti-TNF-α (Mab11) fluorochrome-conjugated antibodies.

Statistical analyses

Results are expressed as percentages or medians (range). OS was defined as the time from registration to death (or date of last follow-up); PFS was defined as the time from registration to first progression. Patients alive without progression were censored at their date of last follow-up. OS and PFS were estimated using the Kaplan–Meier method with Rothman's 95% confidence intervals (95% CI).

For immune parameters, statistical analyses were performed using Prism 5 software (GraphPad, San Diego, CA). P values < 0.05 were considered significant. Groups were compared using Mann–Whitney's test or Wilcoxon matched pairs test where appropriate. For correlation statistics, the Spearman's correlation test was used.

Study approval

All patients enrolled in the trial signed an informed consent prior to conducting any study procedures; according to the guidelines presented in CSET 2008/1437 IDRCB 2008-A1171-5 (NCT01159288).

Trial Registration

CSET 2008/1437 IDRCB 2008-A1171-54; NCT01159288 (clinicaltrials.gov/show/NCT01159288)

Disclosure of potential conflicts of interest

We certify that this phase II trial was not conducted with an industrial partner or a Biotech company.

References

1. Chen DS, Mellman I. Oncology meets immunology: the cancer-immunity cycle. Immunity 2013; 39:1-10; PMID:23890059; http://dx.doi.org/10.1016/j.immuni.2013.07.012
2. Lizee G, Overwijk WW, Radvanyi L, Gao J, Sharma P, Hwu P. Harnessing the power of the immune system to target cancer. Annu Rev Med 2013; 64:71-90; PMID:23092383; http://dx.doi.org/10.1146/annurev-med-112311-083918
3. Kantoff PW, Higano CS, Shore ND, Berger ER, Small EJ, Penson DF, Redfern CH, Ferrari AC, Dreicer R, Sims RB et al. Sipuleucel-T immunotherapy for castration-resistant prostate cancer. New Engl J Med 2010; 363:411-22; PMID:20818862; http://dx.doi.org/10.1056/NEJMoa1001294
4. Pitt JM, Charrier M, Viaud S, Andre F, Besse B, Chaput N, Zitvogel L. Dendritic cell-derived exosomes as immunotherapies in the fight against cancer. J Immunol 2014; 193:1006-11; PMID:25049431; http://dx.doi.org/10.4049/jimmunol.1400703
5. Robbins PD, Morelli AE. Regulation of immune responses by extracellular vesicles. Nat Rev Immunol 2014; 14:195-208; PMID:24566916; http://dx.doi.org/10.1038/nri3622
6. Viaud S, Terme M, Flament C, Taieb J, Andre F, Novault S, Escudier B, Robert C, Caillat-Zucman S, Tursz T et al. Dendritic cell-derived exosomes promote natural killer cell activation and proliferation: a role for NKG2D ligands and IL-15Ralpha. PloS One 2009; 4:e4942; PMID:19319200; http://dx.doi.org/10.1371/journal.pone.0004942
7. Lamparski HG, Metha-Damani A, Yao JY, Patel S, Hsu DH, Ruegg C, Le Pecq JB. Production and characterization of clinical grade exosomes derived from dendritic cells. J Immunol Methods 2002; 270:211-26; PMID:12379326; http://dx.doi.org/10.1016/S0022-1759(02)00330-7
8. Viaud S, Thery C, Ploix S, Tursz T, Lapierre V, Lantz O, Zitvogel L, Chaput N. Dendritic cell-derived exosomes for cancer immunotherapy: what's next? Cancer Res 2010; 70:1281-5; PMID:20145139; http://dx.doi.org/10.1158/0008-5472.CAN-09-3276

9. Escudier B, Dorval T, Chaput N, Andre F, Caby MP, Novault S, Flament C, Leboulaire C, Borg C, Amigorena S et al. Vaccination of metastatic melanoma patients with autologous dendritic cell (DC) derived-exosomes: results of thefirst phase I clinical trial. J Trans Med 2005; 3:10; PMID:15740633; http://dx.doi.org/10.1186/1479-5876-3-10
10. Morse MA, Garst J, Osada T, Khan S, Hobeika A, Clay TM, Valente N, Shreeniwas R, Sutton MA, Delcayre A et al. A phase I study of dexosome immunotherapy in patients with advanced non-small cell lung cancer. J Trans Med 2005; 3:9; PMID:15723705; http://dx.doi.org/10.1186/1479-5876-3-9
11. Pignon JP, Tribodet H, Scagliotti GV, Douillard JY, Shepherd FA, Stephens RJ, Dunant A, Torri V, Rosell R, Seymour L et al. Lung adjuvant cisplatin evaluation: a pooled analysis by the LACE Collaborative Group. J Clin Oncol 2008; 26:3552-9; PMID:18506026; http://dx.doi.org/10.1200/JCO.2007.13.9030
12. Polo V, Besse B. Maintenance strategies in stage IV non-small-cell lung cancer (NSCLC): in which patients, with which drugs? Ann Oncol 2014; 25:1283-93; PMID:24351398; http://dx.doi.org/10.1093/annonc/mdt529
13. Lynch TJ, Bondarenko I, Luft A, Serwatowski P, Barlesi F, Chacko R, Sebastian M, Neal J, Lu H, Cuillerot JM et al. Ipilimumab in combination with paclitaxel and carboplatin as first-line treatment in stage IIIB/IV non-small-cell lung cancer: results from a randomized, double-blind, multicenter phase II study. J Clin Oncol 2012; 30:2046-54; PMID:22547592; http://dx.doi.org/10.1200/JCO.2011.38.4032
14. Segura E, Nicco C, Lombard B, Veron P, Raposo G, Batteux F, Amigorena S, Thery C. ICAM-1 on exosomes from mature dendritic cells is critical for efficient naive T-cell priming. Blood 2005; 106:216-23; PMID:15790784; http://dx.doi.org/10.1182/blood-2005-01-0220
15. Utsugi-Kobukai S, Fujimaki H, Hotta C, Nakazawa M, Minami M. MHC class I-mediated exogenous antigen presentation by exosomes secreted from immature and mature bone marrow derived dendritic cells. Immunol Lett 2003; 89:125-31; PMID:14556969; http://dx.doi.org/10.1016/S0165-2478(03)00128-7
16. Viaud S, Ploix S, Lapierre V, Thery C, Commere PH, Tramalloni D, Gorrichon K, Virault-Rocroy P, Tursz T, Lantz O et al. Updated technology to produce highly immunogenic dendritic cell-derived exosomes of clinical grade: a critical role of interferon-gamma. J Immunother 2011; 34:65-75; PMID:21150714; http://dx.doi.org/10.1097/CJI.0b013e3181fe535b
17. Segura E, Amigorena S, Thery C. Mature dendritic cells secrete exosomes with strong ability to induce antigen-specific effector immune responses. Blood Cells, Mol Dis 2005; 35:89-93; PMID:15990342; http://dx.doi.org/10.1016/j.bcmd.2005.05.003
18. Dhodapkar KM, Gettinger SN, Das R, Zebroski H, Dhodapkar MV. SOX2-specific adaptive immunity and response to immunotherapy in non-small cell lung cancer. Oncoimmunology 2013; 2:e25205; PMID:24073380; http://dx.doi.org/10.4161/onci.25205
19. Steimle V, Siegrist CA, Mottet A, Lisowska-Grospierre B, Mach B. Regulation of MHC class II expression by interferon-gamma mediated by the transactivator gene CIITA. Science 1994; 265:106-9; PMID:8016643; http://dx.doi.org/10.1126/science.8016643
20. Kamper N, Franken S, Temme S, Koch S, Bieber T, Koch N. Gamma-Interferon-regulated chaperone governs human lymphocyte antigen class II expression. FASEB J: Off Pub Federat Am Soc Exp Biol 2012; 26:104-16; PMID:21940994; http://dx.doi.org/10.1096/fj.11-189670
21. Pai RK, Askew D, Boom WH, Harding CV. Regulation of class II MHC expression in APCs: roles of types I, III, and IV class II transactivator. J Immunol 2002; 169:1326-33; PMID:12133955; http://dx.doi.org/10.4049/jimmunol.169.3.1326
22. Pogge von Strandmann E, Simhadri VR, von Tresckow B, Sasse S, Reiners KS, Hansen HP, Rothe A, Boll B, Simhadri VL, Borchmann P et al. Human leukocyte antigen-B-associated transcript 3 is released from tumor cells and engages the NKp30 receptor on natural killer cells. Immunity 2007; 27:965-74; PMID:18055229; http://dx.doi.org/10.1016/j.immuni.2007.10.010
23. Matta J, Baratin M, Chiche L, Forel JM, Cognet C, Thomas G, Farnarier C, Piperoglou C, Papazian L, Chaussabel D et al. Induction of B7-H6, a ligand for the natural killer cell-activating receptor NKp30, in

inflammatory conditions. Blood; 2013; 122:394-404; PMID:23687088; http://dx.doi.org/10.1182/blood-2013-01-481705

24. Semeraro M, Rusakiewicz S, Minard-Colin V, Delahaye NF, Enot DP, Vely F, Marabelle A, Papoular B, Piperoglou C, Ponzoni M, et al. Clinical impact of the NKp30/B7-H6 axis in high-risk neuroblastoma patients. Sci Transl Med 2015; 7:283ra55; PMID:25877893; http://dx.doi.org/10.1126/scitranslmed.aaa2327; in press

25. Platonova S, Cherfils-Vicini J, Damotte D, Crozet L, Vieillard V, Validire P, Andre P, Dieu-Nosjean MC, Alifano M, Regnard JF et al. Profound coordinated alterations of intratumoral NK cell phenotype and function in lung carcinoma. Cancer Res 2011; 71:5412-22; PMID:21708957; http://dx.doi.org/10.1158/0008-5472.CAN-10-4179

26. Al-Shibli K, Al-Saad S, Donnem T, Persson M, Bremnes RM, Busund LT. The prognostic value of intraepithelial and stromal innate immune system cells in non-small cell lung carcinoma. Histopathology 2009; 55:301-12; PMID:19723145; http://dx.doi.org/10.1111/j.1365-2559.2009.03379.x

27. Takanami I, Takeuchi K, Giga M. The prognostic value of natural killer cell infiltration in resected pulmonary adenocarcinoma. J Thorac Cardiovasc Sur 2001; 121:1058-63; PMID:11385371; http://dx.doi.org/10.1067/mtc.2001.113026

28. Reiners KS, Kessler J, Sauer M, Rothe A, Hansen HP, Reusch U, Hucke C, Kohl U, Durkop H, Engert A et al. Rescue of impaired NK cell activity in hodgkin lymphoma with bispecific antibodies in vitro and in patients. Mol Ther: J Am Soc Gene Ther 2013; 21:895-903; PMID:23459515; http://dx.doi.org/10.1038/mt.2013.14

29. Reiners KS, Topolar D, Henke A, Simhadri VR, Kessler J, Sauer M, Bessler M, Hansen HP, Tawadros S, Herling M et al. Soluble ligands for NK cell receptors promote evasion of chronic lymphocytic leukemia cells from NK cell anti-tumor activity. Blood 2013; 121:3658-65; PMID:23509156; http://dx.doi.org/10.1182/blood-2013-01-476606

30. Binici J, Koch J. BAG-6, a jack of all trades in health and disease. Cell Mol Life Sci: CMLS 2014; 71:1829-37; PMID:24305946; http://dx.doi.org/10.1007/s00018-013-1522-y

31. Corduan A, Lecomte S, Martin C, Michel D, Desmots F. Sequential interplay between BAG6 and HSP70 upon heat shock. Cell Mol Life Sci: CMLS 2009; 66:1998-2004; PMID:19357808; http://dx.doi.org/10.1007/s00018-009-9198-z

32. Thress K, Song J, Morimoto RI, Kornbluth S. Reversible inhibition of Hsp70 chaperone function by Scythe and Reaper. EMBO J 2001; 20:1033-41; PMID:11230127; http://dx.doi.org/10.1093/emboj/20.5.1033

33. Massa C, Melani C, Colombo MP. Chaperon and adjuvant activity of hsp70: different natural killer requirement for cross-priming of chaperoned and bystander antigens. Cancer Res 2005; 65:7942-9; PMID:16140966; http://dx.doi.org/10.1158/0008-5472.CAN-05-0377

34. Gastpar R, Gehrmann M, Bausero MA, Asea A, Gross C, Schroeder JA, Multhoff G. Heat shock protein 70 surface-positive tumor exosomes stimulate migratory and cytolytic activity of natural killer cells. Cancer Res 2005; 65:5238-47; PMID:15958569; http://dx.doi.org/10.1158/0008-5472.CAN-04-3804

35. Simhadri VR, Reiners KS, Hansen HP, Topolar D, Simhadri VL, Nohroudi K, Kufer TA, Engert A, Pogge von Strandmann E. Dendritic cells release HLA-B-associated transcript-3 positive exosomes to regulate natural killer function. PloS One 2008; 3:e3377; PMID:18852879; http://dx.doi.org/10.1371/journal.pone.0003377

36. Gross C, Schmidt-Wolf IG, Nagaraj S, Gastpar R, Ellwart J, Kunz-Schughart LA, Multhoff G. Heat shock protein 70-reactivity is associated with increased cell surface density of CD94/CD56 on primary natural killer cells. Cell Stress Chaperon 2003; 8:348-60; PMID:15115287; http://dx.doi.org/10.1379/1466-1268(2003)008%3c0348:HSPRIA%3e2.0.CO;2

37. Gross C, Hansch D, Gastpar R, Multhoff G. Interaction of heat shock protein 70 peptide with NK cells involves the NK receptor CD94. Biol Chem 2003; 384:267-79; PMID:12675520; http://dx.doi.org/10.1515/BC.2003.030

38. Germain RN, Bajenoff M, Castellino F, Chieppa M, Egen JG, Huang AY, Ishii M, Koo LY, Qi H. Making friends in out-of-the-way places: how cells of the immune system get together and how they conduct their business as revealed by intravital imaging. Immunol Rev 2008; 221:163-81; PMID:18275481; http://dx.doi.org/10.1111/j.1600-065X.2008.00591.x

39. Delahaye NF, Rusakiewicz S, Martins I, Menard C, Roux S, Lyonnet L, Paul P, Sarabi M, Chaput N, Semeraro M et al. Alternatively spliced NKp30 isoforms affect the prognosis of gastrointestinal stromal tumors. Nat Med 2011; 17:700-7; PMID:21552268; http://dx.doi.org/10.1038/nm.2366

40. Zornig I, Halama N, Lorenzo Bermejo J, Ziegelmeier C, Dickes E, Migdoll A, Kaiser I, Waterboer T, Pawlita M, Grabe N et al. Prognostic significance of spontaneous antibody responses against tumor-associated antigens in malignant melanoma patients. Int J Cancer 2015; 136:138-51; PMID:24839182; http://dx.doi.org/10.1002/ijc.28980

41. Spisek R, Kukreja A, Chen LC, Matthews P, Mazumder A, Vesole D, Jagannath S, Zebroski HA, Simpson AJ, Ritter G et al. Frequent and specific immunity to the embryonal stem cell-associated antigen SOX2 in patients with monoclonal gammopathy. J Exp Med 2007; 204:831-40; PMID:17389240; http://dx.doi.org/10.1084/jem.20062387